Journal of Sound and Vibration (1999) **225**(3), 515–526
Article No. jsvi.1999.2254, available online at http://www.idealibrary.com on IDEAL®

NOISE CAUSED BY CAVITATING BUTTERFLY AND MONOVAR VALVES

H. Hassis

Ecole Nationale d'Ingénieurs de Tunis, B.P. 37, *Le Belvédère* 1002, *Tunis, Tunisia*

(*Received* 7 *September* 1998, *and in final form* 11 *March* 1999)

An experimental study of the effects of cavitation was carried out through an analysis of cavitating Butterfly and Monovar values. Focus is particularly placed on both unsteady pressure and acoustic pressure fluctuations. In this paper, the effects of cavitation on local fluctuation pressure (turbulence), acoustic propagation (damping and sound velocity), resonance frequencies and level of noise are presented.

1. INTRODUCTION

Industrial piping systems can experience severe low-frequency vibration caused by internal flow of the conveyed fluid. Valves, diaphragms (singularities) … can result in annoying and even unbearable noise and high vibration [1–8]. Prediction methods are needed to design costly piping systems against such risks.

In the case of *single-phase flow*, Gibert [1, 9] showed with experimental investigations that the source of vibration is often related to the unsteady turbulent flow which occurs at any singularities. Pressure fluctuations arising from such flow singularities can be separated into two quite distinct zones: (1) in the downstream region nearby to the singularity location (defined by a length 4–10 times the pipe's diameter, D), the fluctuations of pressure and velocity are dominated by an *unsteady* turbulent field; it cannot excite any low-frequencies vibration of pipes; (2) away from the singularity, the fluctuations of pressure and velocity are dominated by an *acoustic* pressure fluctuation caused by a system of standing waves which oscillate randomly in time; at sufficiently low frequencies, only plane waves should be considered.

In the case of *cavitating flow*, the medium is highly affected by the two-phase aspect of the downstream flow of the cavitating singularity. In fact, the sound velocity becomes very low (about 40 m/s) even for a small void ratio. Such an effect of cavitation occurs in a zone where the flow velocity becomes high and the state pressure in consequently low. For that, the method developed by Gibert [9] has to be improved.

Two valves were chosen for the investigation: the Butterfly valve and the Monovar valve. The Butterfly is one of the oldest types of known valves. Such

0022-460X/99/330515 + 12 $30.00/0

a valve is more convenient due to the advantage of its light weight and the rapidity of its manipulation. Initially, the Monovar valve was developed to reduce cavitation effects. It will be shown that even for such types of valves, the effect of cavitation can also be observed.

This paper describes extensive experimental work carried out at EDF France concerning *cavitating* Butterfly and Monovar valves. The main purpose of this study is to present the effects of cavitation on the unsteady turbulence, the acoustic resonance frequencies, the acoustic pressure fluctuations, and the sound velocity and damping flow in the cavitating flow region.

The analysis of the unsteady turbulence is important because noise sources are directly related to the pressure in this area. The study of the effect of the cavitation on resonance frequencies and acoustic pressure fluctuations gives much information about the geometry of the cavitation area, and the propagation and the damping characteristics of the cavitation medium.

2. EXPERIMENTAL ARRANGEMENT AND EQUIPMENT

2.1. TEST EQUIPMENT

The experiments were performed using a purposedly built test rig, the general layout of which is shown in Figure 1. It was made of a straight stainless-steel tube with internal diameter $D = 200$ mm. The tube was made of three parts to facilitate the installation and the removal of the valves. Great care was taken to ensure that each pipe segment was correctly aligned. The investigation was performed with a Butterfly valve of $\phi 200$ (diameter 200 mm) and with a Monovar valve of $\phi 200$ (diameter 200 mm and with 57 circular orifices). To prevent undesirable vibration, the entire test section shown in Figure 1 was clamped to the floor. At each end, the pipe was connected to a forced water flow loop through rubber tubes, flexible enough to isolate efficiently the test section from external acoustical and mechanical vibrations. The experiments were carried out in a close loop with forced circulation of cold water at a temperature of 20°C. Kistler 2501 sensors were directly mounted at the pipe walls to measure the fluctuating pressure at various locations along the pipes (p_1 to p_{13}; see Figure 1). Table 1 presents the experimental conditions used for Butterfly valves.

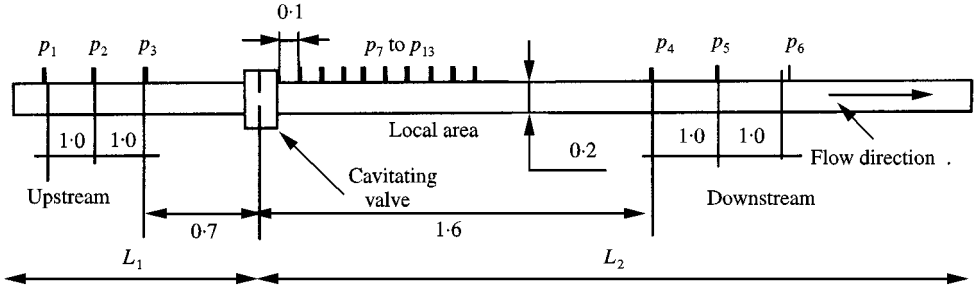

Figure 1. Experimental equipment.

The cavitation number σ is defined as

$$\sigma = (P_d - P_v)/\Delta P, \tag{1}$$

where P_v is the pressure of saturated vapour, P_d is the downstream mean pressure and ΔP is the pressure drop (a list of nomenclature is given in the Appendix).

2.2. DETERMINATION OF THE BOUNDARY CONDITIONS OF THE EXPERIMENTAL TEST SECTION

In order to calculate the transfer function which is used for the acoustic source determination, it is necessary to determine the nature of boundary conditions of the test section. Figures 2(a) and 2(b) show the phase frequency spectrum between a pair of sensors located at two positions on the same side of the valve. Figures 2 allows one to measure the equivalent acoustic impedance at the corresponding pipe end. When the dissipation is small and the impedance is zero, the phase displays a clear step varying from 0 to π or $-\pi$, as actually observed in the present experiment (see Figures 2(a) and 2(b)). The rubber tubes are flexible enough to

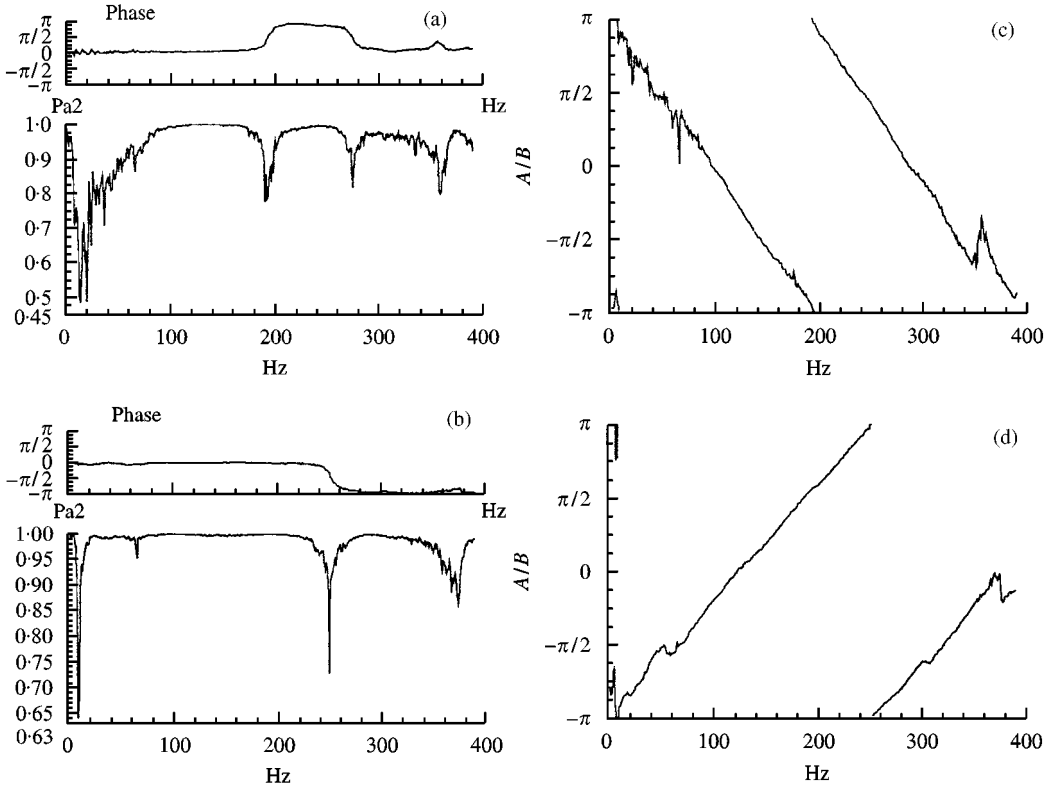

Figure 2. Phase plotted as frequency between two acoustic sensors placed (a) upstream ($\sigma = 0{\cdot}691$), and (b) downstream ($\sigma = 0{\cdot}691$); (c) ratio A/B upstream ($\sigma = 0{\cdot}691$); (d) ratio A/B downstream ($\sigma = 0{\cdot}691$).

absorb the pressure fluctuations. Then the boundary condition is a node of the fluctuating pressure which is located at a position determined with the f_π method given by $f_\pi = c/(2X)$. In this relation f_π is the first frequency associated to the phase change (ranging from 0 to π or $-\pi$), X is the distance between the most remote sensor and the boundary condition and c is the sound velocity. The boundary conditions (upstream or downstream) can be determined also by the *A/B method* (using Figures 2(c) and 2(d): the distance d separating the boundary of the circuit and the first sensor is given by $d = \theta\, c/(4\pi)$, where θ is the slope of the ratio between the incident wave $A(f)$ and reflected wave $B(f)$ (A and B will be defined in Section 5).

The analysis of the results has given the following positions of the pressure nodes:

Length from the valve	Method A/B	Method f_π
Length upstream L_1	5·2 m ($\pm$ 0·2 m)	5·2 m ($\pm$ 0·2 m)
Length downstream L_2	6·02 m ($\pm$ 0·2 m)	6·1 m ($\pm$ 0·2 m)

3. EFFECTS OF CAVITATION ON UNSTEADY FLOW

The effects of the cavitation on the unsteady flow were determined by using the series of tests described in Table 1. Figure 3 shows a set of pressure amplitude spectra obtained downstream of the Butterfly valve for different degrees of cavitation. In Figure 3, one can notice a random broadband signal with a level

TABLE 1

Test conditions; *ΔPm is the measurement pressure drop*, U_0 *is the mean flow velocity*, β *is the opening angle of the valve* (*from* 0 *to* 90°, *measured from vertical position*) *and* σ *is the cavitation number*

Butterfly tests				Monovar tests			
σ	$\beta(^\circ)$	ΔPm	U_0(m/s)	σ	$\beta(^\circ)$	ΔPm	U_0(m/s)
				1·93		1·80	
1·667		1·80		1·65		1·80	
1·314	54	1·88	5·47	1·18	72	2·10	5·25
1·033		1·84		0·82		2·40	
0·691		1·88		0·73		2·45	
				0·52		2·55	
				1·06		2·80	
				0·92		2·80	
0·648		3·55		0·78	54	2·80	3·18
0·394	38·5	3·55	7·03	0·68		2·83	
0·248		3·55		0·44		2·92	
				0·27		3·05	

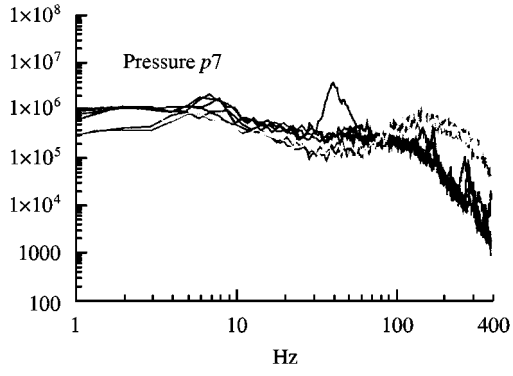

Figure 3. Superposing of local pressure spectra for different σ (Test BUTTERFLY).

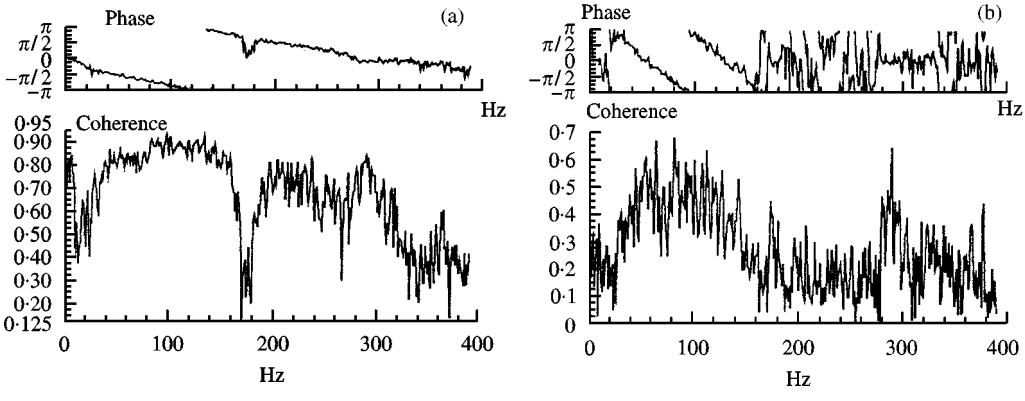

Figure 4. Cross-spectra of local fluctuations (a) sensors $p7$–$p8$ (distance $p7$–$p8 = 10$ cm) ($\sigma = 0{\cdot}648$) (b) sensors $p7$–$p10$ (distance $p7$–$p10 = 30$ cm ($\sigma = 0{\cdot}648$).

decreasing progressively with frequency. However, at the extreme positions of the valve, one can observe the emergence of peaks of low-intensity and high-frequency acoustic resonance.

From the results, one can conclude also that the spectral characteristics of the local pressure fluctuations are little influenced by the cavitation, particularly at low frequencies. However, the level of fluctuation tends to increase when the cavitation number decreases. The cross spectra show that the coherence between the two sensors close to each other remains low (see Figure 4). This indicates that the turbulence structure remains in the small-scale domain. This is not surprising because one does not expect cavitation to organize flow on a large scale.

4. EFFECTS OF CAVITATION ON ACOUSTIC FLUCTUATION PRESSURE (CONSIDERED AS PLANE WAVES)

4.1. GENERAL CHARACTERISTICS OF THE SPECTRA OF ACOUSTIC RESPONSE

The spectra of autocorrelation given by the sensors located upstream and farther downstream look different from those observed immediately downstream of the

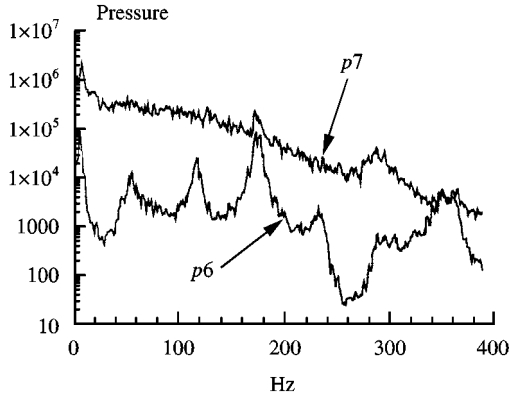

Figure 5. Superposing of an acoustic and a local fluctuations pressure ($p6$ and $p7$); $\sigma = 0{\cdot}248$.

valve (see Figure 5). The level of the acoustic fluctuations is weaker than that of the local pressure fluctuations. In general, the ratio of the typical variations is equal to 5. The spectra of acoustic fluctuations show resonance peaks which depend on the circuit's geometry, on the boundary conditions and on the degree of cavitation σ (σ including the characteristics of the permanent flow). It should be remembered that in non-cavitating flow, they are not dependent on characteristics of the permanent flow. Similarly, the spectra of cross correlation between the two acoustic sensors and the two local sensors have very different characteristics. As we have seen in the previous section, the local fluctuations have a weak coherence (typically lower than 0·5) when the distance between the two sensors is greater than one pipe diameter D. On the other hand, the acoustic fluctuations show areas of high coherence (typically greater than 0·9) independent of the distance between the two sensors. The phase function is mainly characterized by a succession of degrees having values near either 0 or π (see Figures 2(a) and 2(b)).

4.2. UNCOUPLING BETWEEN UPSTREAM AND DOWNSTREAM IN THE CASE OF MONOVAR VALVE

For tests carried out with the Monovar valve, the pressure spectra upstream and downstream do not show the same frequencies (see Figure 6). This uncoupling may be explained by the development of shock waves (the sound velocity becomes lower than that of the flow). In fact, the frequencies upstream (multiples of 125 Hz) correspond to those of a pipe with length equal to L_1 (the upstream length of the pipe used) and limited by two nodes of pressure. In this case, the frequencies f_n are given by

$$f_n = \frac{nc}{2L_1} = \frac{n1300}{2 * 5{\cdot}2} = n\,125 \text{ Hz}. \tag{2}$$

From Figure 6, one can observe that the upstream level of fluctuations is lower than the downstream level.

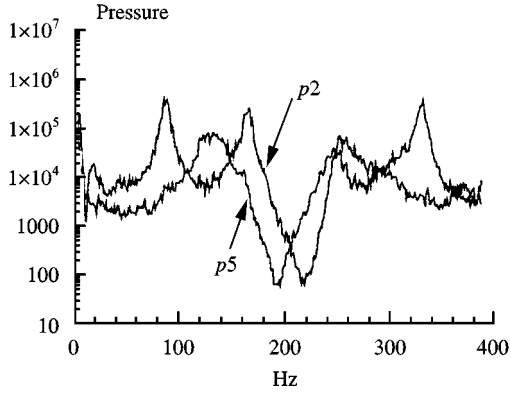

Figure 6. Uncoupling upstream – downstream: sensor $p2$ and $p5$; $\sigma = 0{\cdot}248$. (MONOVAR test).

TABLE 2

Effects of the cavitation on the acoustic resonance frequencies

Butterfly tests				Monovar tests				
σ	f_1	f_2	f_3	σ	f_1 upstream	f_1 downstream	f_2 upstream	f_2 downstream
1·667	58	119	178	0·52	125	20	250	80
1·314	58	119	178	0·73	125	25	250	105
1·033	52	119	171	0·82	125	25	250	105
0·691	40	110	142	1·18	35	35	110	110
				1·65	45	45	120	120
				1·93	45	45	120	120
0·648	50	119	168	0·27	25	25	250	80
0·394	43	113	144	0·44	40	40	105	105
0·248	22	60	114	0·68	42	42	120	120
				0·78	42	42	118	118
				0·92	55	55	120	120
				1·06	58	58	120	120

4.3. EFFECT OF CAVITATION ON RESONANCE FREQUENCIES

In non-cavitating flow, the acoustic frequency number n of a pipe limited by two pressure nodes is $f_n = nc/(2L)$, where L is the total length of the circuit. Theoretically, resonance frequencies are multiples of 58 Hz (the precision is about 5 Hz).

Table 2 shows the evolution of the three first measured acoustic frequencies (f_1, f_2, f_3) as a function of the cavitation number σ. From Table 2, it can be seen that when the cavitation number decreases, the resonance frequencies decrease.

5. EFFECT OF CAVITATION ON DAMPING AND ON SOUND VELOCITY

By using linearized local continuity and momentum equations averaged with time, the equation governing the linear acoustic waves, in straight pipe, is given by [4]

$$(1 - M^2)\frac{\partial^2 p}{\partial x^2} - 2\frac{U_0}{c^2}\left[\frac{\partial^2}{\partial t}\frac{p}{\partial x} + \frac{\partial U_0}{\partial x}\frac{\partial p}{\partial x}\right] - \frac{1}{c^2}\left[\frac{\partial^2 p}{\partial t^2} + 2\frac{\partial p}{\partial t}\frac{\partial U_0}{\partial x}\right] = 0, \qquad (3)$$

where p is the fluctuating acoustic pressure, U_0 is the mean flow velocity, x is the curvilinear abscissa and M is the Mach number defined by $M = U_0/c$.

The propagative nature of solutions is well known. For instance, in a uniform fluid, the Fourier transform of the harmonic plane waves with pulsation $\omega = 2\pi f$ propagating along the Ox-axis has the general form

$$p(x,f) = A(f)\mathrm{e}^{-\mathrm{i}(k_+)x} + B(f)\mathrm{e}^{i(k_-)x}, \qquad (4)$$

where A is the incident wave propagating in the positive direction of the flow, B is the reflected wave propagating in the opposite direction, and k_+ and k_- are respectively the wave numbers of the A wave and the B wave.

The unknown variables of the problem are $A(f)$, $B(f)$ and c. The numerical signals $A(f)$ and $B(f)$ are composed of m values. Wave velocity represents an additional unknown. Thus, one has $2m + 1$ unknown variables. Pressure measurements give m data. In order to solve the problem, one needs to have three sensors placed at equal distance and to compute the wave velocity by calculating the half-sum of the transfer functions between the sensors on each side (p_1 and p_3) and the central one (p_2). This gives

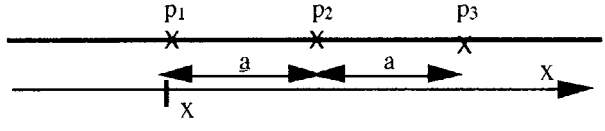

$$\frac{1}{2}\frac{p_1(x,f) + p_3(x + 2a,f)}{p_2(x + a,f)} = \mathrm{e}^{-\mathrm{i}(k_+)a} + \mathrm{e}^{\mathrm{i}(k_-)a}. \qquad (5)$$

If the Mach number is small (case of non-cavitation flow), one obtains a real cosine function:

$$\frac{1}{2}\frac{p_1(x,f) + p_3(x + 2a,f)}{p_2(x + a,f)} = \cos\frac{(\omega a)}{c}. \qquad (6)$$

Application of equation (6) at upstream and downstream positions gives a sound velocity exceeding 1300 m/s. The experimental curve corresponds well to the theoretical curve (see Figure 7(a)).

However, in the cavitating region, the strong damping and the high Mach number invalidate the simple model, defined by equation (6) (see Figure 7(b)). When the damping is not weak, the wave number is complex with a real part k^r and an

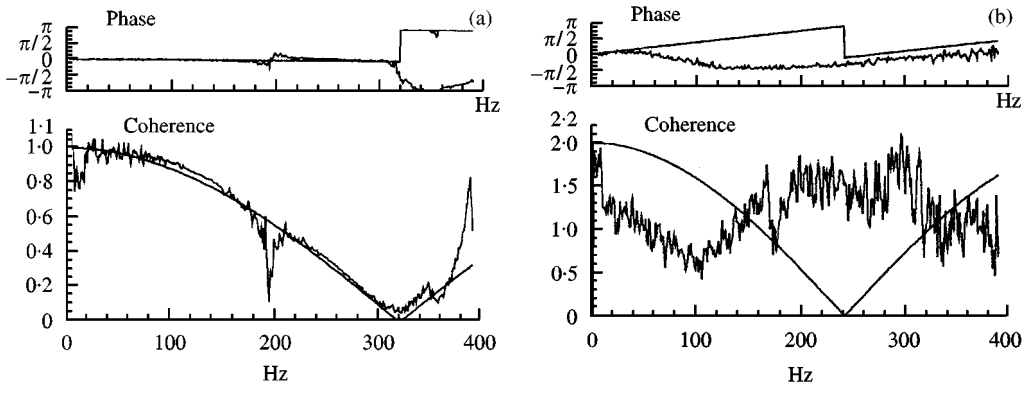

Figure 7. Identification of sound velocity in (a) one phase area ($\sigma = 1{\cdot}667$), (b) cavitation area ($\sigma = 0{\cdot}248$).

imaginary part k^i. Equation (6) becomes

$$\frac{1}{2}\frac{p_1(x,f) + p_3(x+2a,f)}{p_2(x+a,f)} = \cos(k^r_+ a)\mathrm{e}^{k^i_+ a} + \cos(k^r_- a)\mathrm{e}^{-k^i a} + \mathrm{i}\,\sin(k^r_+ a)e^{k^i_+ a} - \mathrm{i}\,\sin(k^r_- a)\mathrm{e}^{-k^i_- a}. \quad (7)$$

6. ADJUSTMENT OF CAVITATION AREA PARAMETERS

To adjust the parameters which characterize the cavitation area, it is necessary to take into account the Doppler effect (equation (3)). By applying a matrix transfer formulation, the resonance frequencies of a circuit are defined by the equation

$$\cos\frac{\omega L_c}{C_c(1-M^2)}\sin\frac{\omega(L_1+L_2)}{c} + \sin\frac{\omega L_c}{C_c(1-M^2)}\left[\frac{C_c}{c}\cos\frac{\omega L_1}{c}\cos\frac{\omega L_2}{c} - \frac{c}{C_c}\cos\frac{\omega L_1}{c}\cos\frac{\omega L_2}{c}\right] + \mathrm{i}\,MC_c\sin\frac{\omega L_2}{c}\sin\frac{\omega(L_2-L_1)}{c} = 0, \quad (8)$$

where C_c and L_c are respectively the sound velocity and the length of the cavitating region. The imaginary term has a small effect and one can suppose that the resonance frequencies are given by the annulment of the real part of this expression. The evolutions of the first and the third resonance frequencies as a function of C_c and L_c are respectively given in Figures 8(a) and 8(b).

An example of adjustment of the sound velocity C_c and the length of the cavitating zone L_c of the Butterfly valve is given in Table 3 where different valves of Cc and Lc such as calculated frequencies, with these values, coincide with the measured frequencies. The void fraction α associated to each case is determined by

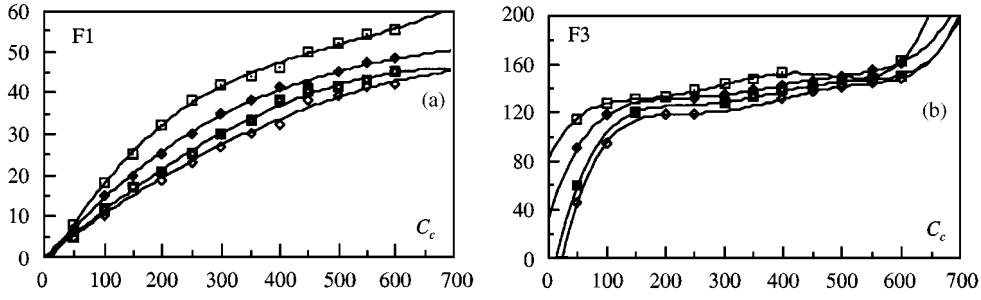

Figure 8. Evolution of (a) the first resonance frequency and (b) the third resonance frequency, as functions of C_c and L_c. ⊡ $L_c = 0{\cdot}25$ m, ◆ $L_c = 0{\cdot}50$ m, ■ $L_c = 0{\cdot}75$ m, ◇ $L_c = 1{\cdot}0$ m.

TABLE 3

Estimated frequencies (Butterfly valve)

σ	C_c (m/s)	L_c (m)	Calculated frequencies	Void fraction
1·667	M			
1·314	M			
1·033	550	0·25	52; 115; 227;	3·35E-4
0·691	400	0·50	41; 115; 142;	6·66E-4
	450	0·75	40; 115; 140;	5·10E-4
	550	1·00	41;115;143;	3·25E-4
	600	1·25	41;115;142;	2·65E-4
0·648	500	0·25	52; 115; 165;	4·15E-4
0·394	450	0·50	42; 115; 145;	5·10E-4
	500	0·75	41; 115; 144;	5·00E-4
	550	1·00	41; 115; 143;	3·25E-4
0·248	250	1·50	20;78;125;	1·80E-3
	200	1·75	17;58;110;	2·80E-3

using the relation

$$C_c = \left[\frac{1-\alpha}{C_l^2}\left(1-\alpha+\alpha\frac{\rho_g}{\rho_l}\right)+\frac{\alpha}{C_g^2}\left(\alpha+(1-\alpha)\frac{\rho_l}{\rho_g}\right)\right]^{-1/2}, \tag{9}$$

where C_l and C_g are respectively the sound velocity in the liquid and in the gas, and ρ_l and ρ_g are respectively the mass density in the liquid and in the gas. Table 3 gives the void fraction values.

7. CONCLUSION

The effects of the cavitation have been shown by investigating a Butterfly valve and a Monovar valve in cavitating flow. The following comments can be obtained from experimental results presented here.

The spectral properties of the local pressure fluctuations are slightly influenced. However, the level of fluctuation increases at the high frequencies when the cavitation number decreases.

As for the acoustic effects, cavitation induces a decrease in the resonance frequencies and an increase if the level of noise.

A non-coupling between upstream and downstream of the pipe is observed in Monovar valve tests. More tests should be done to explain this phenomena.

In the cavitation area, the wave number becomes a complex one. The real part contains the damping effect of cavitation and the imaginary part contains the sound velocity (the propagation wave velocity).

In order to determine the transfer function or the response of circuits to acoustic sources, the characteristics of cavitation area (Cc and Lc) are estimated in the case of our cavitation tests. More tests should be done to define a clear relationship between the cavitation number and this parameters.

ACKNOWLEDGEMENTS

The author is very grateful to E. Dueymes, A. Boyer and J. F. Lauro of EDF Chatou France for providing the experimental data presented in the paper. This work was supported by EDF and SEREME (France).

REFERENCES

1. R. J. Gibert and F. Axisa 1978 *B.N.E.S. Keswick*. Flow induced vibrations of piping systems.
2. J. A. Chada, D. E. Hobson, A. Marshall and D. H. Wilkinson 1980 *ASME PVP Conference San Francisco USA August* 12–15 1980, *Vol.* 41, 125–138. Acoustic source properties of governor valves.
3. W. K. Blake 1986 *Mechanics of Flow induced Sound and Vibration*. New York: Academic Press.
4. R. J. Gibert 1998 *Vibrations des structures*: *interaction avec les fluides*, *sources d'excitations aléatoires*. Edition EYROLLES.
5. H. Hassis 1990 Doctorat de l'Université de Paris 6-Février 1990. Contribution à l'étude des lignes de tuyauteries excitées par des singularités d'écoulement en régime monophasique ou cavitant.
6. H. Hassis, F. Axisa, F. Hareux and T. Valin 1990 *Rapport CEA DEMT/90.131*. Vibrations de tuyauteries excitées par une singularité en écoulement interne. Etude de diaphragme simples et étagés à orifice unique en écoulement d'eau non-cavitant et cavitant.
7. N. Kugou 1996 *1996 Fluids Engineering Division Conference*, *Vol.* 1 ASME. Cavitation characteristics of restriction orifices.
8. P. S. Addison *et al.* 1997 *Journal of Fluids Engineering* **119**. An experimental investigation into the breakdown of low Reynolds number pulsed flows at a pipe orifice.
9. R. J. Gibert 1974 *Doctorat es-science 1974*. Etude expérimentale de deux singularités d'un circuit.

APPENDIX: NOMENCLATURE

$A(f)$	incident wave
$B(f)$	reflected wave

c	sound velocity
C_c	sound velocity in cavitation zone
C_g	sound velocity in the gas phase
C_l	sound velocity in the liquid phase
D	diameter of pipe
f	frequency
$f_1 .. f_n$	frequency number $1, \ldots, n$
f_π	phase ranging from 0 to π or $-\pi$
k	wave number
L	total length of pipe
L_1	pipe's upstream length
L_2	pipe's downstream length
L_c	length of cavitation area
M	Mach number
P_d	downstream mean pressure
P_v	vapour pressure
P_1, p_n	sensor number $1, \ldots, n$
U_0	mean flow velocity
x	curvilinear abscissa
α	void fraction
β	valve opening angle
ΔP	pressure drop
ΔPm	measured pressure drop
ω	pulsation
ρ	mass density of fluid
ρ_g	mass density of gas
ρ_l	mass density of liquid
σ	cavitation number
θ	slope of A/B